FEBS Letters 564 (2004) 136–142 FEBS 28289

Kinetic analysis of operator binding by the *E. coli* methionine repressor highlights the role(s) of electrostatic interactions

Isobel D. Lawrenson[1], Peter G. Stockley*

Astbury Centre for Structural Molecular Biology, School of Biochemistry and Molecular Biology, University of Leeds, Leeds LS2 9JT, UK

Received 9 January 2004; accepted 19 March 2004

First published online 29 March 2004

Edited by Hans Eklund

Abstract MetJ is a member of the ribbon-helix-helix class of DNA-binding proteins whose affinity for operators is apparently controlled by an unprecedented long-range electrostatic effect from the tertiary sulphur atom of its co-repressor, *S*-adenosyl methionine. We report here the results of kinetic assays of DNA binding with MetJ mutant proteins having altered net charges. The results (a) suggest that MetJ locates its operators via a sliding mechanism, (b) support the idea that electrostatic steering is important in the initial DNA binding event and (c) highlight the sensitivity of this system to electrostatic effects.

Key words: Methionine repressor; Operator binding; Surface plasmon resonance; *Escherichia coli*

1. Introduction

The *Escherichia coli* methionine repressor, MetJ, controls transcriptional initiation at at least eight operons regulating genes for biosynthetic enzymes [1] and was the first structurally characterised member of the ribbon-helix-helix (RHH) (see Fig. 1a) family of DNA-binding proteins [2–4]. MetJ exists as a homo-dimer in solution. Binding of a co-repressor, *S*-adenosylmethionine (AdoMet), to the face of each monomer opposite the DNA-binding motif increases the affinity for operators by at least 100-fold [5–7]. This is believed to be due to an unprecedented long-range electrostatic effect, the 'electric genetic switch', emanating from the positive charge on the tertiary sulphur atoms of the AdoMets [8,9]. Operator regions to which the holo-repressor binds consist of between two and five tandem repeats of an 8-bp sequence known as a met-box (consensus = dAGACGTCT). The minimal stable repression complex in vitro comprises two MetJ dimers bound to two adjacent met-boxes [3,5,10]. High-resolution crystal structures and functional studies [2,3,10–13] have suggested how sequence specificity in this system is achieved. Sequence-specific contacts to the edges of DNA base pairs in the major grooves of the operator are made by amino acid side chains from the anti-parallel β-ribbon [3,12]. Sequence-dependent distortions of the phosphodiester backbone also play important roles, allowing increased contact between the DNA and the repressors, and orientating the repressors so that adjacent dimers can make protein–protein interactions via their A-helices.

Since the protein has a distinct charge distribution across its surface, the C-terminal helical face being largely negatively charged, whilst the β-ribbon face is mildly positive, and because the co-repressor effect appears solely to be electrostatic in origin, we expected this protein to be extremely sensitive to electrostatic effects caused by mutation. We have therefore created a series of site-directed mutants to explore the role(s) of surface charges in operator binding. All the mutations have the result of decreasing the overall negative charge (−6 for wild-type) on the repressor (Fig. 1a) and are distributed on the β-ribbon face (Q44K and N53K); in the 'middle' of the protein (E79K and S81K), or on the co-repressor-binding face (D72R/E94R). Additionally, in order to investigate the possible role(s) of the C-terminal helix that is not present in other RHH proteins, a protein truncated at position 83 (E83stp) has been produced. This position corresponds roughly to the C-terminal residue of the P22 Arc repressor, another member of the RHH family [4,14]. The mutant proteins have been over-expressed, purified and their kinetics of binding to DNA determined in vitro using an optical biosensor [9,15,16].

2. Materials and methods

2.1. Mutagenesis and protein purification

Site-directed mutagenesis was performed using standard techniques [12]. E83stp was expressed in BL21DE3 (F^- *ompT* $r_B^- m_B^-$ (DE3), Cm^r) [17]. All other mutants were over-expressed in the *E. coli metJ*$^-$ strain GT1008 (*xyl*, *ilvA*, Δ*lacX74*, *srl*::Tn*10*, *met185am*) [18,19]. Mutant repressors were purified and quantitated as described [9,12] or by a slight modification using a mimetic green affinity matrix (Affinity Chromatography) and size exclusion chromatography.

2.2. Biosensor experiments

The biosensor experiments were carried out using a BIACORE2000 instrument to monitor kinetics by surface plasmon resonance (SPR) as previously described [9,15,16,20]. The buffer used was TKE (20 mM Tris–HCl pH 7.4, 250 mM KCl, 0.5 mM EDTA, 0.0005% v/v Tween 20), unless otherwise stated. The repressor was diluted in the experimental buffer containing saturating levels of co-repressor. To measure the dissociation in the presence of co-repressor, an injection command was used which allows two consecutive injections of sample with no intermediate delay. The first injection was of repressor plus co-repressor (30 μl) and the second was of co-repressor alone (30 μl), i.e. the DNA binding and dissociation of the holo-repressor was measured. At the end of each experiment the DNA surface was regenerated by an injection of 15 μl 0.05% w/v sodium dodecyl sulfate (SDS). A flow rate of 30 μl/min was used at 25°C and the response values were recorded at 0.2-s intervals. Binding experiments were carried out in triplicate and the data were corrected for background binding by

*Corresponding author. Fax: (44)-113-343 3092.
E-mail address: stockley@bmb.leeds.ac.uk (P.G. Stockley).

[1] Present address: 62, Smith Street, Brunswick West, Vic. 3055, Australia.

0014-5793/04/$30.00
doi:10.1016/S0014-5793(04)00336-9

subtracting the sensorgrams produced by injecting identical protein samples across an underivatised, adjacent reference flow cell. The data were analysed using the linear kinetic analysis in the BIAevaluation software package [21,22]. The reaction between immobilised DNA and repressor was assumed to follow pseudo-first-order kinetics described by the equation

$$dR/dt = k_{ass}C\,(R_{max}-R)-k_{diss}R \quad (1)$$

where dR/dt is the rate of complex formation, k_{ass} is the apparent association rate constant, k_{diss} is the apparent dissociation rate constant, R is the amount of bound repressor, R_{max} is the maximum repressor binding capacity of the surface, and C is the repressor concentration in the solution.

Rearranging Eq. 1 shows that the derivative of the binding curve is a linear function of the response.

$$dR/dt = k_{ass}CR_{max}-(k_{ass}C+k_{diss})R$$

In theory k_{ass} and k_{diss} can be calculated by plotting dR/dt vs R. Determination of R_{max} however requires prohibitively high concentrations of protein. To circumvent this problem plots of dR/dt are made for a range of protein concentrations. The slopes k_s, from each of these lines are plotted against C where

$$-k_s = k_{ass}C + k_{diss}$$

The slope of this line yields the apparent association rate constant and the y-intercept the apparent dissociation rate constant. However, for low values of k_{diss} the intercept is too close to the origin to allow accurate determination. During the dissociation phase, when buffer plus effector has replaced the repressor solution, the concentration of repressor effectively drops to zero if there is no significant rebinding and then Eq. 1 becomes

$$dR/dt = -k_{diss}R \text{ or } \ln(R_0/R_n) = k_{diss}(t_n-t_0)$$

where R_0, R_n, t_0 and t_n are values obtained along the dissociation curve at times 0 and n. The apparent dissociation rate constant can be obtained from the slope of the line $\ln(R_0/R_n)$ vs (t_n-t_0). To minimise complications due to rebinding as the concentration of complex falls we only analysed the initial phase of these dissociation curves. The ratio of the apparent rate constants allows the apparent equilibrium constant to be calculated, $K_{d'} = k_{diss}/k_{ass}$. When values of $K_{d'}$ were

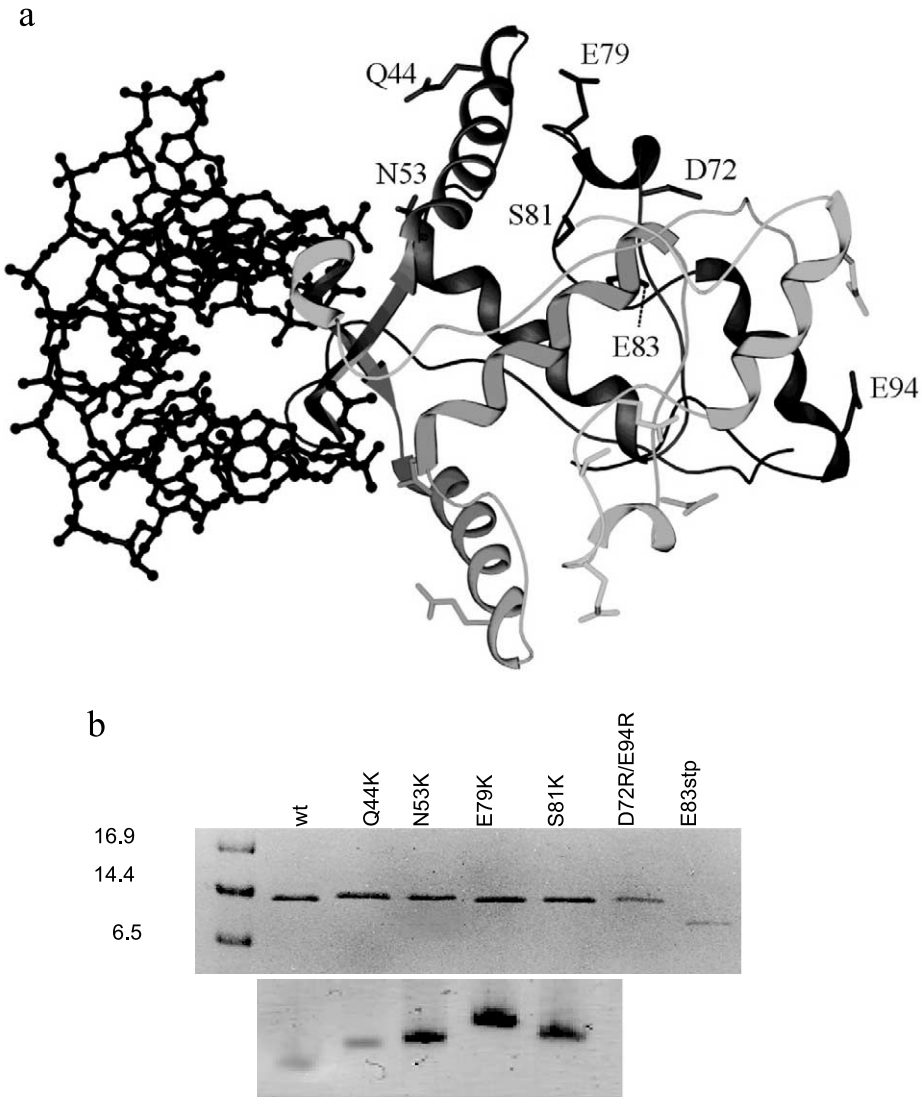

Fig. 1. Characterisation of the mutant repressors studied. a: Cartoon representation of a single repressor dimer bound to a single met-box (framework model) within the higher-order complex (PDB 1cma) [3]. The positions of the mutated side chains are shown as stick models on a ribbon backbone of a single repressor dimer (chains in light and dark grey). AdoMet omitted for clarity. b: Gel characterisation of mutant repressors. Top: sodium dodecyl sulfate–polyacrylamide gel electrophoresis, labels to the left are molecular weight standards in kDa; bottom: native gel.

calculated from k_{ass} and k_{diss} the errors of $K_{d'}$ ($EK_{d'}$) were calculated from the errors of k_{ass} (Ek_{ass}) and k_{diss} (Ek_{diss}) using:

$$EK_{d'} = K_{d'}\sqrt{\left(\frac{Ek_{diss}}{k_{diss}}\right)^2 + \left(\frac{Ek_{ass}}{k_{ass}}\right)^2}$$

Under the assay conditions used here we have shown previously [9,15,16] that this is a valid description of the formation of the MetJ repression complex, even though it is not a simple 1:1 species. The resultant $K_{d'}$ values ($\sim$2.5 nM) from SPR assays compare well to those derived by nitrocellulose filter binding, gel retardation [5] or fluorescence anisotropy (unpublished) that all yield values $\sim$4 nM.

3. Results and discussion

3.1. Mutagenesis and protein purification

Previously we showed that two single amino acid mutations (E94R and D72R) give rise to proteins that exhibit unexpected DNA-binding behaviour [12]. In order to examine these effects in more detail the double mutant (E94R/D72R) was produced, together with point mutations to introduce additional positive charges throughout the protein, as discussed above. Both neutral and acidic side chains were chosen for mutation leading to net charge changes of +2 to +4 per repressor dimer. The double and truncated mutants have net charge changes of +8 and +6, respectively. Conventional site-directed mutagenesis protocols were used and the mutant repressor genes expressed in a *metJ*$^-$ strain and purified to homogeneity. The behaviour of the mutant proteins during chromatography was generally consistent with expectations based on their net charge changes. Purified proteins were analysed on both SDS and native polyacrylamide gels and showed the expected mobilities under these conditions (Fig. 1b). The mobilities of the double and truncated mutants could not be compared in non-denaturing conditions because their overall charges are either opposite to that of the wild-type protein (−6) or zero. The molecular mass of the E83stp mutant protein was confirmed by mass spectrometry.

The circular dichroism spectra of a number of the mutant proteins were essentially super-imposable with the wild-type between 190 and 230 nm [23]. The thermal stability of a number of the purified proteins was also determined using differential scanning calorimetry [24]. Mutation resulted in only very modest (2–4°C) changes in T_m compared to wild-type (53.2°C), which is significantly above the temperature of the experiments described here, suggesting that dimer assembly/folding was also largely unaffected. This conclusion has been confirmed for two of the mutants (Q44K and N53K) by structure determination [10,25].

3.2. The co-repressor requirements of the mutant repressors

Repressor binding was studied to three DNAs: (1) a 79-bp fragment that encompasses two tandem, consensus met-boxes flanked by two 8-bp anti-met-boxes [5], that are designed to reduce extended binding outside the operator site (PCA); (2) an identical 79-bp fragment in which the 16 bp corresponding to the two met-boxes were replaced with 16 random nucleotides, i.e. a degenerate mixture (16N) and (3) a 71-bp fragment in which the two met-boxes were replaced by an 8-bp single met-box (SMB). These fragments were amplified from templates using polymerase chain reaction with a primer carrying a terminal biotin residue. The products were immobilised on commercial streptavidin-containing sensor chips and repressor binding analysed using the SPR assay described previously [9,15,16].

Prior to determining the DNA affinities for the mutants, the co-repressor requirement of each protein was determined [9] by monitoring the interaction of 200 nM repressor dimer with the PCA operator in the presence of varying AdoMet concentrations (62 μM–4 mM). DNA binding by all the mutant repressors was enhanced by the presence of AdoMet and they all had different DNA-binding properties compared to wild-type repressor. At 1 mM AdoMet, however, all of the mutants had roughly similar RU responses and so this concentration was adopted for all subsequent binding assays. Note that the SPR assay measures the association and dissociation of the holo-repressor minimising any differences due to altered AdoMet binding by the mutants.

3.3. The mechanism of operator site location

The mechanism of operator site location by MetJ was then investigated. For sequence-specific DNA-binding proteins this is believed to occur via two processes. The first is a collisional interaction between the protein from solution and a DNA fragment containing the specific binding site. The second is a rearrangement of this complex to form the specifically bound species via a facilitated diffusion event, resulting in formation of the repression complex more rapidly than allowed by simple diffusion. The latter can occur by non-sequence-specific, one-dimensional sliding along the DNA duplex, three-dimensional hopping along the duplex, where the protein is never fully released from the effect of the DNA, or by intersegment transfer in which the protein transiently binds two DNA duplexes simultaneously [26]. These mechanisms can be distinguished experimentally by measuring the apparent association rate (k_{ass}) of the wild-type protein with the PCA fragment at differing salt concentrations. Table 1 lists the apparent k_{ass} and k_{diss} values obtained, whilst Fig. 2 shows a plot of log(k_{ass}) vs log[KCl]. The latter has the typical 'bell shape' expected for a sliding mechanism [26]. Sliding is also sensitive to the length of the DNA fragment containing the target site, so the experiments were repeated with fragments encompassing the PCA operator but 121 or 248 bp in length. The k_{ass} values in both cases increased significantly, as expected for sliding, but were so close to the detection limit of the BIAcore that further analysis in terms of a plot of k_{ass} vs [KCl] was not possible. Thus although MetJ is a dimer in solution [27] and is believed to form the higher-order complexes only on the DNA, it behaves in a manner similar to

Table 1
Salt dependence of DNA-binding kinetics by MetJ

KCl (mM)	k_{diss} ($\times 10^{-3}$ s^{-1})	k_{ass} ($\times 10^{5}$ M^{-1} s^{-1})	$K_{d'}$ (nM)
150	5.5 ± 1.0	6.0 ± 1.0	9.16 ± 2.26
200	5.2 ± 1.0	12.0 ± 1.4	4.33 ± 0.97
250	6.9 ± 0.5	20.0 ± 1.0	3.45 ± 0.30
300	7.4 ± 0.8	12.0 ± 6.0	6.16 ± 3.16
350	5.8 ± 0.4	8.0 ± 0.6	7.25 ± 0.74
400	4.2 ± 0.9	6.0 ± 0.3	7.00 ± 1.54
450	5.2 ± 0.6	6.0 ± 1.0	8.66 ± 1.76

The apparent rate constants were determined as described in Section 2. ± represents the standard error calculated by the software and was used throughout to calculate errors on derived values, i.e. $K_{d'}$. The data represent the results of multiple injections of at least six protein concentrations, in triplicate.

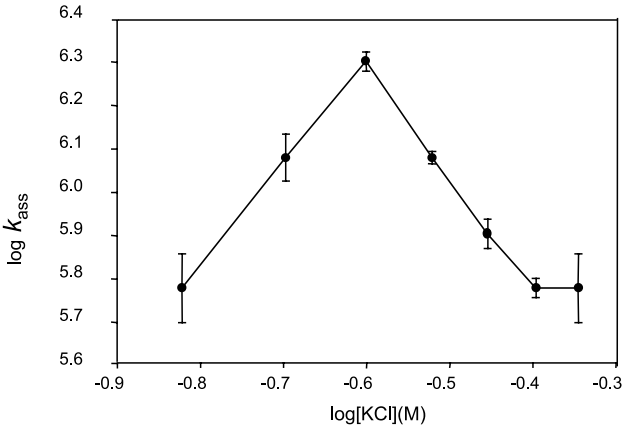

Fig. 2. Effect of salt concentration on binding of wild-type repressor. Plot of log(k_{ass}) vs log([KCl]) for the binding of wild-type MetJ to the PCA fragment. Units of k_{ass} are M^{-1} s^{-1}.

other DNA-binding proteins by locating its sequence-specific target after initially binding non-specifically and then sliding on the DNA. Note, estimation of the k_{ass} value, via a modified Smoluchowski equation [26], yields a result close to those observed under SPR assay conditions for the 79-bp fragment. This is the expected result on a short DNA fragment where the effect of sliding is limited. The values obtained with the longer DNAs are consistent with an increasing contribution of sliding.

In principle, MetJ could also participate in intersegment transfer because the C-terminal helices have homology to the first helix of a helix-turn-helix motif and, in a dimer, they are located ~34 Å apart, leading to an initial proposal that they might be part of the DNA-binding motif [2]. However, it was not possible to operate the SPR assay in conditions to detect such intersegment transfer. Instead we determined the affinity of the truncated mutant to see if the loss of the C-terminal helices affected binding. In the binding buffer containing 250 mM KCl, E83stp rapidly lost DNA-binding activity. This problem was overcome by increasing the KCl concentration to 350 mM, under which conditions the truncated protein bound specifically to the PCA fragment consistent with formation of a dimer of dimers. Sensorgrams were also recorded for wild-type protein in this buffer (Fig. 3). The apparent kinetic constants for binding (Table 2) suggest that removal of the C-terminal helices has little or no effect on operator binding under these conditions and effectively rules out intersegment transfer as part of the mechanism of operator site location. It also suggests that the overall charge on the protein (0 for the E83stp mutant) has little effect on DNA binding. In 350 mM KCl, however, the affinity of the wild-type repressor was decreased four-fold due both to a reduced k_{ass} and an increased k_{diss}, confirming that the interaction has an electrostatic component.

3.4. The effect of charge changes on operator binding kinetics and specificity

SPR sensorgrams were then recorded (left panels of Fig. 3) for the binding of all the other mutant proteins to all three target sites over a wide range of protein concentrations (60–2000 nM MetJ dimer). As reported previously [9,15,16] for the wild-type protein, the protein–protein co-operativity in this system is such that linear kinetic assumptions can be used. This also appears to be true for the mutants (right panels of Fig. 3). In all cases the dissociation phases were biphasic as

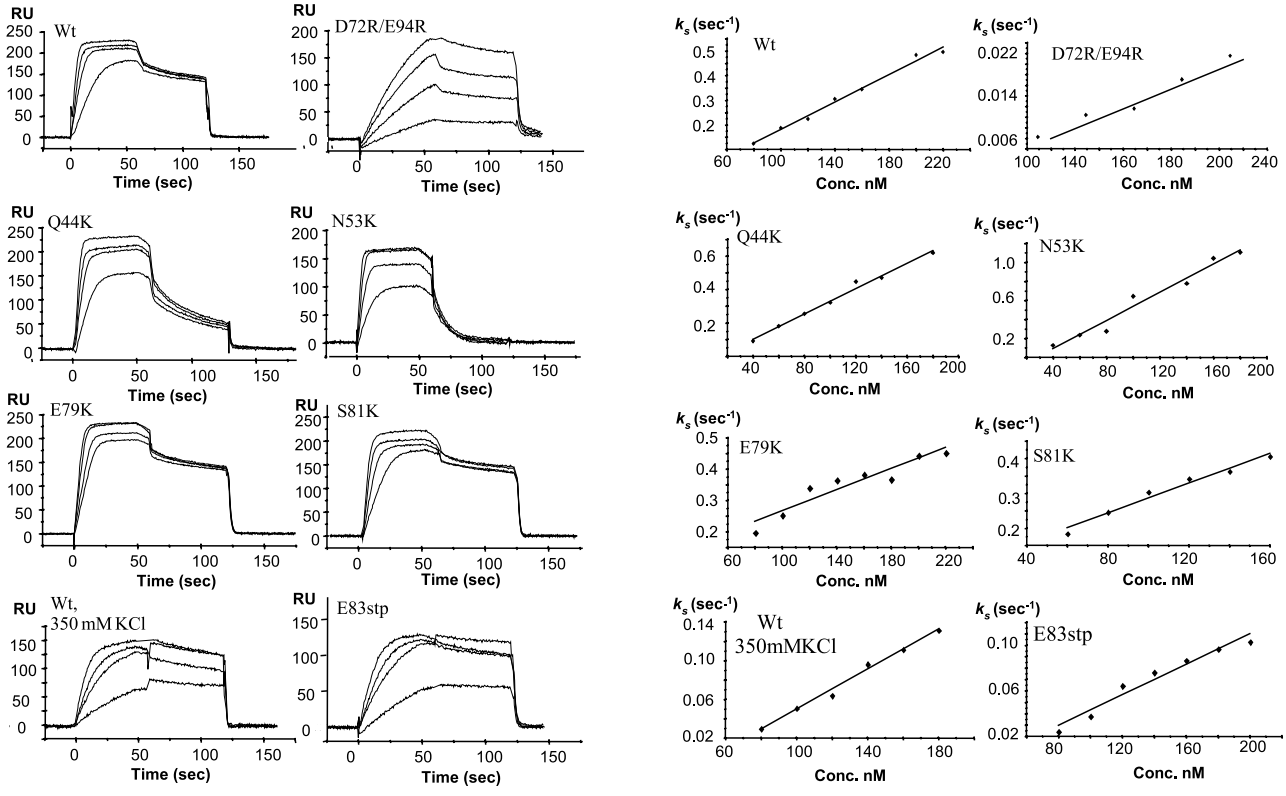

Fig. 3. SPR kinetic analysis. Left: Corrected sensorgrams showing the binding of wild-type and mutant repressors to PCA DNA. The sensorgrams are from one of three binding experiments used to calculate the kinetic constants. Right: Linear plots of k_s vs concentration.

Table 2
Kinetics of operator binding by charge-change mutants

Repressor	Net charge change	k_{diss} ($\times 10^{-3}$ s^{-1})	k_{ass} ($\times 10^{6}$ M^{-1} s^{-1})	$K_{d'}$ (nM)	Relative affinity (%)
250 mM KCl					
Wild-type	0	8.5 ± 0.6	3.2 ± 0.27	2.66 ± 0.29	100
β-strand mutants					
Q44K	+2	14 ± 1.4	3.3 ± 0.46	4.24 ± 0.73	63
N53K	+2	48 ± 4.0	7.2 ± 1.70	6.67 ± 1.67	40
'Middle'					
E79K	+4	10 ± 1.4	1.7 ± 0.10	5.88 ± 0.89	45
S81K	+2	10 ± 0.6	1.7 ± 0.32	5.88 ± 1.16	45
C-helix face					
D72R/E94R	+8	7.6 ± 0.2	0.18 ± 0.01	42.22 ± 2.60	6
350 mM KCl					
Wild-type	0	12.5 ± 2.9	1.1 ± 0.03	11.36 ± 2.65	100
C-helix face					
E83stp	+6	12.9 ± 4.4	0.9 ± 0.10	14.33 ± 4.89	80[a]
SMB binding[b]					
Q44K	+2	120 ± 16	1.55 ± 0.04	77.42 ± 10.51	–
N53K	+2	124 ± 10	0.8 ± 0.07	155.00 ± 18.44	–

The apparent rate constants for the interaction of the wild-type and mutant repressors with the PCA fragment are listed. The approximate relative affinity is given as a percentage of wild-type repressor under the same experimental conditions. The data were derived from a single sensor chip allowing comparison of binding to the identical DNA fragment.
[a]Relative to wild-type in 350 mM KCl.
[b]In 250 ml KCL.

observed previously, due to the effect of increased rebinding as dissociation proceeds [9,15]. The initial phases of the dissociation plots were used to calculate values for k_{diss}. k_{ass} was calculated from the linear plots of k_s vs concentration. The resultant apparent kinetic constants are listed in Table 2. With the exceptions of the double and truncated mutants, whose binding curves failed to reach saturation under the experimental conditions, it was possible to estimate the relative stoichiometries of the complexes being formed with the PCA fragment by comparison to the wild-type repressor. In each case, the data were consistent with formation of a dimer of dimers.

In most cases the effects of mutation on affinity were relatively modest. Although mutant N53K had a lower apparent affinity than wild-type, it actually had a higher on-rate (~2×). Its apparent off-rate was, however, much greater (~6×). This is consistent with the X-ray structure of the N53K–PCA complex [25] which shows that the introduced lysine side chain makes a fortuitous inter-dimer contact with glutamine 44 of its neighbour, suggesting that formation of the higher-order complex is more favourable and hence k_{ass} is higher. The reduced stability of the complex formed, as judged from the sharply increased off-rate, may reflect the loss of extended DNA–protein hydrogen bonds from one of the repressor loops which becomes less ordered.

Q44K has essentially wild-type affinity consistent with previous gel retardation and filter-binding assays [10]. Crystal structures show that the lysine in this position can make an additional contact to the DNA phosphodiester backbone, stabilising the presumed intermediate of a single dimer bound to a single met-box site [10,11]. It also reduces the apparent protein–protein co-operativity by partially trapping a species that needs to undergo conformational change to form the higher-order complex. As expected there is a significant contribution to overall binding energy from forming the larger complex resulting in a significantly higher off-rate in the single dimer complex. Unexpectedly, N53K also binds to the SMB site. The X-ray structure of the higher-order complex in this case [25] does not explain this behaviour but perhaps the lysine at position 53 can make a stabilising contact to the backbone of the DNA, analogous to that seen with Q44K, in the intermediate complex. Mutants E79K and S81K had similar affinities that were approximately half that of the wild-type protein. This is due primarily to effects on the on-rate. The double mutant, D72R/E94R, was the most affected with an affinity ~15× lower than wild-type. Once again this is primarily the result of changes to the on-rate.

Since the C-terminal helix face of the repressor is not apparently directly involved in operator binding, these effects of mutations away from the β-ribbon DNA-binding face must arise from an indirect mechanism. A plausible explanation for these phenotypes comes from a consideration of the charge distribution over the surface of the protein. As mentioned above, MetJ is an extremely bipolar molecule [8]. Such a charge distribution might assist the orientation of the repressor during the initial collision with DNA, facilitating the interaction of the β-ribbon motif with the major groove. The E79K, S81K and D72R/E94R mutations increase the positive charge away from the N-terminal face thus disrupting this effect. This would lead to the predictions that the on-rates for such mutant repressors would be lower than for wild-type, whilst the off-rates might be unaffected because the charges distal to the N-terminal face are too far away to be detected at the DNA-binding motif. Precisely such behaviour is seen (Table 2). Since simple removal of the C-terminal helices yielding a repressor with fewer negatively charged residues on that face fails to show a similar effect, it is clear that the creation of positively charged patches away from the N-terminal face is the origin of the reduced affinity.

With the exceptions of Q44K and N53K binding to the SMB target, mutant binding to the SMB and 16N targets did not follow linear kinetics, although under the experimental conditions the SPR responses of Q44K, N53K, E79K and S81K appeared to reach saturation. Thus it is possible to examine what appears to be non-specific DNA binding in the SPR assay. Relative-binding plots were therefore constructed (Fig. 4) in which the extent of binding of each mutant to the target at each concentration could be compared directly to that of wild-type. At the lower protein concentrations all

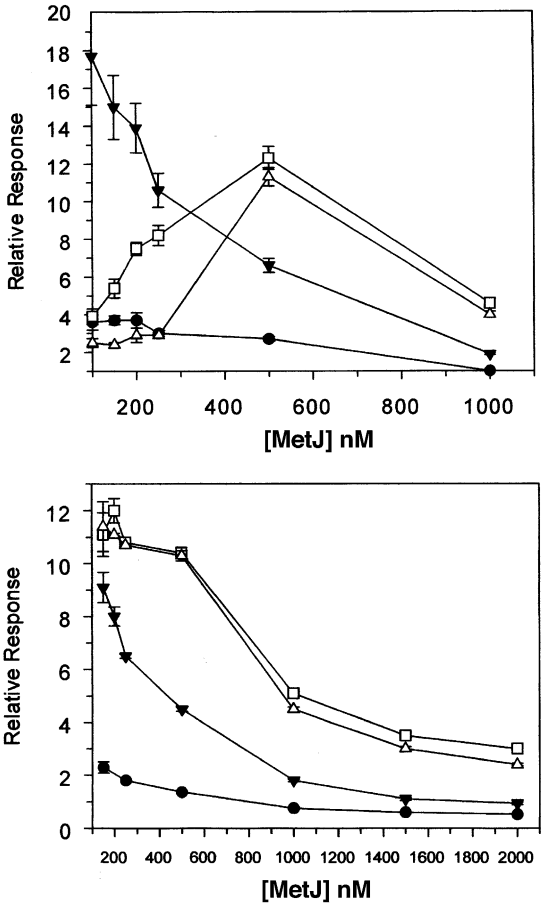

Fig. 4. The relative-binding plots for the SMB (top) and 16N (bottom) targets. Each data point is the mean value obtained from three repetitions of the experiment. The error bars show the standard deviation from the mean, where the error bars are not visible they are smaller than the size of the graphing symbol. Protein concentrations are shown as nM dimer.

the mutants showed increased binding relative to the wild-type repressor, suggesting that all the charge-change mutants have reduced sequence specificity. This is consistent with our earlier explanation of the phenotypes of the D72R and E94R mutant repressors in filter-binding assays [12].

Charge-change mutants have been reported in other repressors, such as TrpR and lambda cI, leading to altered phenotypes both in vivo and in vitro [28,29]. These effects have been determined to be due to alterations in oligomerisation, protein folding and/or ligand binding. Here the use of the SPR assay, which allows rapid analysis of co-repressor dependence, the kinetics of DNA binding and stoichiometry, has allowed us to characterise a range of such mutants in the MetJ system in greater detail than before. In the MetJ system an electrostatic interaction appears to control the co-repressor effect but this represents only $\sim$20% of the overall binding energy [10]. The effect is a long-range one since the AdoMet binds on the face distal to the DNA-binding motif. However, the AdoMet binding site appears to screen the charge on the tertiary sulphur from the solvent, thus maximising this long-range effect. Simply adding positively charged amino acid residues that are in contact with solvent to this face does not remove the need for co-repressor. However, as expected for a system whose operator affinity is controlled by charge–charge interactions, addition of positively charged side chains can lead to dramatic effects. On the DNA-binding face this can stabilise intermediates in complex formation.

Mutations away from the N-terminal face appear to cause effects indirectly by disruption of events on the pathway to operator site location. Collisional electrostatic steering of complex formation is well documented for protein–protein and protein–ligand interactions [30] in which an initial encounter complex rearranges to a stable species depending on the mutual orientation of its components. Both the rate of collision and the orientation of the partners can be affected by long-range electrostatic interactions. Such effects would explain the changes to the on-rate observed here. Once orientated and non-specifically bound to DNA we assume that sliding to the operator would occur normally. To our knowledge this is the first time that such clear evidence for such an effect has been reported for a DNA-binding protein. The in vitro phenotypes defined here will be vital for the interpretation of transcriptome assays with MetJ mutants (Marincs et al., in progress).

Acknowledgements: We thank Drs Chi Trinh for Fig. 1a, Iain Manfield for helpful comments on the manuscript, Isabelle Saint-Girons for gifts of MetJ expression constructs and the *metJ*$^-$ strain, Jeff Keen, Richard Virden and Ms Denise Ashworth for help with mass spectrometry, circular dichroism and oligonucleotide syntheses, respectively. We also thank Prof. Alan Cooper for differential scanning calorimetry data. This work was supported by the UK BBSRC.

References

[1] Old, I.G., Phillips, S.E.V., Stockley, P.G. and Saint-Girons, I. (1991) Prog. Biophys. Mol. Biol. 56, 145–185.
[2] Rafferty, J.B., Somers, W.S., Saint-Girons, I. and Phillips, S.E.V. (1989) Nature 341, 705–710.
[3] Somers, W.S. and Phillips, S.E.V. (1992) Nature 346, 586–590.
[4] Phillips, S.E.V. (1994) Annu. Rev. Biophys. Biomol. Struct. 23, 671–701.
[5] Phillips, S.E.V., Manfield, I., Parsons, I.D., Davidson, B.E., Rafferty, J.B., Somers, W.S., Margarita, D., Cohen, G.N., Saint-Girons, I. and Stockley, P.G. (1989) Nature 341, 711–715.
[6] Cooper, A., McAlpine, A. and Stockley, P.G. (1994) FEBS Lett. 348, 41–45.
[7] Hyre, D.E. and Spicer, L.D. (1995) Biochemistry 34, 739–761.
[8] Phillips, K. and Phillips, S.E.V. (1994) Structure 2, 309–316.
[9] Parsons, I.D., Persson, B., Mekhalfia, A., Blackburn, M. and Stockley, P.G. (1995) Nucleic Acids Res. 23, 211–216.
[10] He, Y.Y., Garvie, C.W., Elworthy, S., Manfield, I.W., McNally, T., Lawrenson, I.D., Phillips, S.E.V. and Stockley, P.G. (2002) J. Mol. Biol. 320, 39–53.
[11] Garvie, C.W. and Phillips, S.E.V. (2000) Struct. Fold. Des. 8, 905–914.
[12] He, Y.Y., McNally, T., Manfield, I., Navratil, O., Old, I.G., Phillips, S.E.V., Saint-Girons, I. and Stockley, P.G. (1992) Nature 359, 431–433.
[13] Wild, C.M., McNally, T., Phillips, S.E.V. and Stockley, P.G. (1996) Mol. Microbiol. 21, 1125–1135.
[14] Raumann, B.E., Rould, M.A., Pabo, C.O. and Sauer, R.T. (1994) Nature 367, 754–757.
[15] Parsons, I.D. and Stockley, P.G. (1997) Anal. Biochem. 254, 82–87.
[16] Stockley, P.G., Baron, A.J., Wild, C.M., Parsons, I.D., Miller, C.M., Holtham, C.A.M. and Baumberg, S. (1998) Biosensors Bioelect. 13, 637–650.
[17] Studier, F.W., Rosenberg, A.H., Dunn, J.J. and Dubendorff, J.W. (1990) Methods Enzymol. 185, 60–89.
[18] Saint-Girons, I., Belfaiza, J., Guillou, Y., Perrin, D., Guiso, N., Bârzu, O. and Cohen, G.N. (1986) J. Biol. Chem. 261, 10936–10940.

[19] Davidson, B.E. and Saint-Girons, I. (1989) Mol. Microbiol. 3, 1639–1648.
[20] Fägerstam, L.G. and O'Shannessy, D.J. (1993) in: Handbook of Affinity Chromatography, Vol. 63 (Kline, T., Ed.), pp. 229–252, Marcel Dekker, New York.
[21] O'Shannessy, D.J., Bringham-Burke, M., Soneson, K.K., Hensley, P. and Brooks, I. (1993) Anal. Biochem. 212, 457–468.
[22] Karlsson, R., Roos, H., Fagerstam, L. and Persson, B. (1994) Methods; A Companion to Methods in Enzymology, Vol. 6, pp. 99–110, Academic Press, New York.
[23] He, Y.-Y. (1992) PhD Thesis, University of Leeds, Leeds.
[24] Johnson, C.M., Cooper, A. and Stockley, P.G. (1992) Biochemistry 31, 9717–9724.
[25] Wang, S.-F. (1997) PhD Thesis, University of Leeds, Leeds.
[26] von Hippel, P.H. and Berg, O.G. (1989) J. Biol. Chem. 264, 675–680.
[27] Smith, A.A., Greene, R.C., Kirby, T.W. and Hindenach, B.R. (1985) Proc. Natl. Acad. Sci. USA 82, 6104–6108.
[28] Reedstrom, R.J., Martin, K.S., Vangala, S., Mahoney, S., Wilker, E.W. and Royer, C.A. (1996) J. Mol. Biol. 264, 32–45.
[29] Nelson, H.C. and Sauer, R.T. (1985) Cell 42, 549–558.
[30] Janin, J. (1997) Proteins 28, 153–161.